NONLINEAR STUDY OF RAYLEIGH-TAYLOR INSTABILITY IN THIN FILMS PAST A POROUS LAYER

N. Rudraiah[*], C. Wagner[**], G. S. Evans[**] AND R. Friedrich[**]

[*]*UGC-DSA Centre in Fluid Mechanics, Department of Mathematics, Bangalore University (Central College), Bangalore 560 001, India*

[**]*Lehrstuhl für Fluidmechanik, TU München, Germany*

The linear and nonlinear Rayleigh-Taylor instability in a viscous fluid layer of finite thickness bounded above by a porous layer and below by a rigid surface, have been studied based on approximations in effect similar to lubrication and Stokes approximations. The linear problem is studied analytically while the nonlinear problem is investigated using both, harmonic evolution of the interface and numerical integration.

It is shown that the nature of the linear stability curve is controlled by both the porous-slip parameter β and the thickness h of the fluid layer while its shape is controlled only by the ratio of the surface tension γ, and the normal stress term δ. Comparing the results of linear and nonlinear analysis we found that nonlinear effects are significant only for small values of h. In general, we observed that the change in the nature of the interface (i.e., the nominal surface) is related to changes of the value of the slip parameter α.

Key Words : Rayleigh-Taylor Instability; Thin Films; Porous Layer; Stones Approximations

1. INTRODUCTION

The phenomenon of instability of the interface between a heavy fluid supported by a lighter fluid, known as Rayleigh-Taylor- instability (hereafter denoted by RTI) has been studied extensively starting from Rayleigh[1] and Taylor[2]. A detailed account of RTI is given by Chandrasekhar[3]. More recently, this problem has attracted considerable interest (see Sharp[4], and Mikaelian[5] and references therein) because of its natural occurrence and of its importance in science, engineering and technology. It plays a crucial role in the areas of inertial confinement fusion (CIF) target design, astrophysics and geophysics (see Bernstein and Book[6], Sharp[4]).

In ICF design where an ablative driven medium implodes compressing the material ahead of the ablation front to high densities, RTI plays a significant role (see Mikaelian[7]). On the other hand Rudraiah *et al.*[8] pointed out that a magnetic field applied obliquely to the interface between two kinds of electrically conducting viscous fluids exerts a stabilizing influence on the configuration. The literature mentioned above (being by no means an exhaustive survey of the work on this subject, but rather a representative sample of the enormous effort in this area) is concerned with the RTI between two different fluids, but much attention has not been given to its study either in two different fluid saturated porous media or in a fluid bounded by a fluid saturated porous layer.

There exists a large body of literature dealing with the subject of flow, heat and mass transfer in a fluid region bounded by a porous layer (see Rudraiah[9, 10], Prasad[11]). The problem in this case is to specify a suitable boundary condition at the interface between the fluid saturated porous layer, called interior flow and the fluid layer, called exterior flow.

The usual conditions are the continuity of velocity and surface streses at this boundary. However, it is not possible to apply these conditions when the interior flow is governed by Darcy's law which is of reduced order as compared to the Navier-Stokes equations.

To overcome this difficulty, Beavers and Joseph[12] postulated a boundary condition

$$\frac{\partial u}{\partial y}\bigg|_{y=h} = \frac{\alpha}{k^{1/2}}(u_B - Q) \qquad \qquad \text{... (1)}$$

known as BJ-slip condition. Here u is the local average tangential velocity in the exterior flow, u_B is the slip velocity at $y = h$,

$$Q = -\frac{k}{\mu}\frac{\partial p}{\partial x} \qquad \qquad \text{... (2)}$$

is the tangential velocity in the interior flow given by Darcy's law, k the permeability of the porous layer, $\frac{\partial p}{\partial x}$ the pressure gradient in the x-direction and α the slip coefficient, a dimensionless constant depending on the local geometry of the interstices. Beavers and Joseph[12] conducted experiments to verify this BJ-slip condition and they found the values of α ranging from 0.1 to 4.

Taylor[13] performed experiments with grooved plates as a well-characterized model for an idealized porous medium to verify the BJ-slip condition and found values of α from 1.308 to > 7 as the thickness of the grooves changed. His experimental results showed agreement with the theoretical ones of Richardson[14]. Saffman[15] gave a theoretical justification for the BJ-slip condition and showed that the condition could be derived in the form

$$u = \frac{k^{\frac{1}{2}}}{\alpha}\frac{\partial u}{\partial y}\bigg|_{y=h} + O(k). \qquad \qquad \text{... (3)}$$

Saffman[15] notes that the detailed analysis of the transition region and precise definition of the nominal surface are necessary to describe the slip velocity u_b to higher order in k. Further, the precise location of the nominal surface will affect the value of α. Rudraiah[16] has improved the BJ-slip condition to make it valid for finite thickness of the porous layer. He derived from first principles, a slip-condition of the form

$$\frac{\partial u}{\partial y} = \left(\frac{\lambda''}{k}\right)^{\frac{1}{2}}\left[\frac{\varepsilon\lambda''Q}{\sinh(\lambda'H)} + (u_b - Q)\coth(\lambda'H)\right], \qquad \qquad \text{... (4)}$$

where H is the thickness of the porous layer, ε the porosity (cf. eq. (8)), $\lambda' = (\alpha''k)^{-\frac{1}{2}}$ and λ'' are viscosity parameters. This equation reduces to the BJ-slip condition in the limit of $H \rightarrow \infty$.

From this discussion it is clear that the slip parameter depends on the nature of the interface. The instability of the interface between porous medium and free flow has hardly been studied in the literature. One of the motivations of this paper is, therefore, to analyze the effect of the slip

parameter on the RTI. In other words, the results of this paper are both of academic and technological interest.

The academic interest is to know how sensitive the interface will be to variations of the slip parameter and the structure of a porous medium. The other academic interest is to know the evolution of passive and active interfaces which helps to understand the continental drift and the volcanic activities. The technological interest is in the study of material science, particularly involving localized deformation and failure of solids. Brown[17] has employed a RTI configuration to study the polymer failures using viscous creeping flow in the absence of a porous layer. He has pointed out that polymer failures occur normally by the formation and growth of planar defects (crazes) that look like cracks. The two faces of these defects are joined by many fibrils with the environmental fluid present between them. The bundle of these fibrils may be modelled as a porous medium and the environmental fluid in it may be regarded as flow through porous media bounded on one side by a natural fluid, i.e., air. When the crazing is accelerated by the presence of a plasticizing fluid, it is likely that the thin layer of material adjacent to the porous layer will be plasticized and will experience a slip. it may then undergo a RTI-like instability. The problem of particular interest is the effect of slip at the interface, of the permeability of the bundle of fibrils and of the thickness of the layer on the instability wavelength.

Another important application of RTI past a porous layer is in the design of an effective porous wall insulation. Wetting of porous insulation has been noticed to persist despite many preventive devices (see Ognewicz and Tien[18]). This is attributed to the unavoidable formation of openings arising from faulty insulation and aging. The wetting phenomenon is generally believed to cause a significant deterioration in the performance of wall insulation.

This is generally a complex multi-dimensional problem involving a liquid in a porous medium bounded by air. The interface between the liquid (wet) zone and air (dry) zone undergoes RTI-phenomena and should be taken care of in designing an effective insulation. This problem involves both heat and moisture transport in porous media in addition to momentum transport due to gravity and capillary action. This momentum transport sets up a slip between a thin dry layer and wet saturated porous layer. A solution to this general problem is not attempted at this stage; instead we deal only with the effect of the slip parameter on the stability of the interface between these two zones. We consider in this paper both one-dimensional and two-dimensional RTI phenomena in a thin film bounded above by a porous layer using the slip condition proposed by Saffman[16]

The plan of this paper is as follows: The basic equations and the corresponding boundary conditions are discussed in section 2 using the approximations proposed by Babchin et al.[19] Section 3 is devoted to the study of both linear and nonlinear one-dimensional RTI problems. The linear problem is solved analytically whereas the nonlinear problem needs numerical integration based on 4th order central differences in space and time. The two-dimensional linear RTI-problem is discussed in section 4 using an analytical method. Section 5 contains a discussion and general conclusions.

2. MATHEMATICAL FORMULATION

The physical problem to be studied is shown in Fig.1 There is a two-dimensional horizontal fluid-porous medium composite system with a heavy fluid (of density ρ_p) in the porous region of height H supported by a light fluid (of density ρ_f) in a region of height h bounded by a rigid material at $y = 0$. The coordinates x and y indicate horizontal and vertical positions, respectively. The interface between the fluid-saturated porous medium and the fluid is described by $\eta(x, t)$. When it is completely flat we recover the nominal surface, $\eta = 0$, $y = h$. We denote by u and v the

velocity components in x and y directions, respectively. The fluids are assumed to be Newtonian, viscuous and incompressible. Between the two fluids there exists the surface tension γ. The relevant parameters are the fluid viscosity μ, the permeability k of the porous layer, the slip parameter, α, at the interface, the fluid surface tension γ and the gravitational force $\delta = g(\rho_p - \rho_f)$. The basic equations for the fluid-porous medium composite system are :
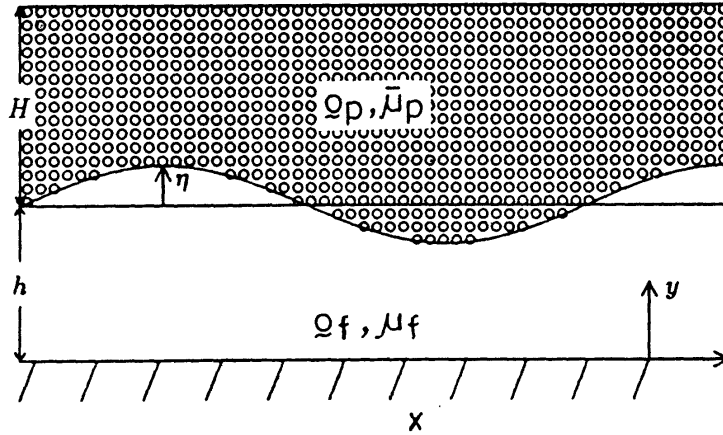

FIG. 1. Physical configuration

The conservation of momentum

$$\rho_f \left[1 + X_p \left(\frac{\rho_p}{\varepsilon \rho_f} - 1 \right) \right] \frac{\partial q}{\partial t} + \rho_f \left[1 + X_p \left(\frac{\rho_p}{\varepsilon^2 \rho_f - 1} \right) \right] (q \cdot \nabla) q$$

$$= - \nabla_p + \mu_f \left[1 + X_p \left(\frac{\mu_p}{\mu_f} - 1 \right) \right] \nabla^2 q - X_p \left[\frac{\mu_f}{k} + \frac{\rho C_b}{\sqrt{k}} |q| \right] q \qquad \text{... (5)}$$

and the conservation of mass for an incompressible fluid

$$\nabla \cdot q = 0 \qquad \text{... (6)}$$

$$X_p = \begin{cases} 0, & \text{for the fluid layer} \\ 1, & \text{for the porous layer.} \end{cases} \qquad \text{... (7)}$$

Here $q = (u, v)$ is the velocity vector, $\bar{\mu}_p$ the effective viscosity, ε the porosity, C_b the inertia factor (i.e. the drag coefficient) of the porous medium and all other quantities are as described above. Eq. (5) is the conservation of equation of momentum written in a general form using the binary number X_p in such a way that this equation gives the Navier-Stokes equation when $X_p = 0$ and the Darcy-Lapwood-Forchheimer-Brinkman equation when $X_p = 1$.

This form is useful for numerical computation in so far as we get the combined numerical results. Assigning suitable values for X_p, we obtain the results either for fluid layers or for porous layers. The parameters ε, K and C_b are defined as (cf. Vortmeyer and Schuster[20]:

$$\varepsilon = \varepsilon_0 \left[1 + C \exp \left(1 - \frac{2K}{d_p} \right) \right],$$ ... (8)

$$K = 1.75 \frac{(1 - \varepsilon)^2}{\varepsilon^2 d_p^2}$$ ... (9)

and $$C_b = \frac{1.75}{\sqrt{1.75}} \varepsilon^{1.5}.$$ ... (10)

Here ε_0 is the effective porosity, the average value of which is 0.4. C is an empirical constant to be adjusted according to ε_0, and d_p is the particle diameter. The solution to this general problem is not attempted at this stage.

To understand the physics of the problem described above, it is simplified using the following assumptions (Babchin et al.[19]) :

(a) The fluid in the porous layer is saturated and immobile and its effect on the properties is negligible.

(b) The thickness of the porous layer H, is assumed to be larger than the film thickness h. That is

$$h \ll H$$ ... (11)

(c) The density of the fluid in the porous layer is higher than that in the film region. That is

$$\rho_p > \rho_f$$ ... (12)

(d) The Strouhal number S, which measures the ratio of the local rate of change due to temporal changes to the convective rate of change in eq. (5) is small. That is

$$S = \frac{\lambda}{(TU)} \ll 1$$ ... (13)

Here $U = \frac{V}{\lambda}$ is the characteristic velocity and $v = \frac{\mu_f}{\rho_f}$ the kinematic viscosity. The characteristic length λ is

$$\lambda = \left(\frac{\gamma}{\delta} \right)^{\frac{1}{2}}, \text{ the characteristic time } T = \frac{\mu_f \gamma}{\chi^2 \delta^2}$$ ... (14)

and

$$\delta = g(\rho_p - \rho_f)$$ ... (15)

(e) The film perturbation Reynolds number R, defined as

$$R = \frac{Uh^2}{\lambda v}$$ ... (16)

is assumed to be small. That is

$$R \ll 1.$$ ... (17)

(f) The interface elevation η is considered small in comparison with the film thickness h. That is

$$\frac{\eta}{h} \ll 1 \qquad\qquad\qquad\qquad\qquad\qquad\qquad\qquad\qquad\qquad \dots (18)$$

Using the conditions (11) to (18) many terms in the basic equations are estimated to be negligible to leading order. For example, conditions (13) and (16) allow us to neglect temporal and convective derivatives in eq. (5).

The required boundary conditions are:

The no-slip conditions

$$u = v = 0 \quad \text{at} \quad y = 0, \qquad\qquad\qquad\qquad\qquad\qquad\qquad \dots (19)$$

the slip condition at the interface

$$\frac{\partial v}{\partial x} + \frac{\partial u}{\partial y} = \frac{\alpha}{\sqrt{k}} u \quad \text{at} \quad y = h. \qquad\qquad\qquad\qquad\qquad \dots (20)$$

The normal stress condition

$$p = -\delta\eta - \gamma\frac{\partial^2 \eta}{\partial x^2} + \mu\frac{\partial v}{\partial t} \quad \text{at} \quad y = h. \qquad\qquad\qquad\qquad \dots (21)$$

The kinematic condition

$$v = \frac{\partial \eta}{\partial t} + u\frac{\partial \eta}{\partial x} \qquad\qquad \text{at} \quad y = h, \qquad\qquad\qquad\qquad \dots (22)$$

where the second term on the right-hand side of eq. (22) will be ignored in dealing with linear analysis.

3. COMBINED LUBRICATION AND STOKES APPROXIMATIONS

In addition to approximations (11) to (18) we use the approximation that the ratio of the film disturbance y-scale to the x-scale is small. That is

$$\frac{h}{\lambda} \ll 1 \ . \qquad\qquad\qquad\qquad\qquad\qquad\qquad\qquad\qquad\qquad \dots (23)$$

Here λ is the characteristic perturbation x-scale given by (14). Condition (23) allows us to neglect the x-derivatives in the film in comparison to their y-counterparts. Approximations (11) to (18) and (23) are, in effect the combined lubrication and Stokes approximations. Using these approximations, equations (5) to (6) and the boundary and surface conditions (19) to (22) take the form

$$\frac{\partial^2 u}{\partial y^2} = \frac{1}{\mu}\frac{\partial p}{\partial x} , \qquad\qquad\qquad\qquad\qquad\qquad\qquad\qquad \dots (24)$$

$$\frac{\partial p}{\partial y} = 0 \qquad\qquad\qquad\qquad\qquad\qquad\qquad\qquad\qquad\qquad \dots (25)$$

and $$\frac{\partial u}{\partial x} + \frac{\partial v}{\partial y} = 0. \qquad \qquad \qquad \cdots (26)$$

The corresponding boundary and surface conditions are

$$u = 0 \text{ at } y = 0, \qquad \qquad \cdots (27)$$

$$\frac{\partial u}{\partial y} = \frac{\alpha}{\sqrt{k}} u \text{ at } y = h, \qquad \qquad \cdots (28)$$

$$p = -\delta\eta - \gamma\frac{\partial^2\eta}{\partial x^2} \qquad \qquad \cdots (29)$$

and $$v(h) = \frac{\partial\eta}{\partial t} + u\frac{\partial\eta}{\partial x} \qquad \qquad \cdots (30)$$

We use the approximation

$$u(\eta) \approx u(h) + \frac{\partial u}{\partial y}\Big|_{y=h} \eta = \left(1 + \alpha\sigma\frac{\eta}{h}\right)u(h) \qquad \cdots (31)$$

$$v(\eta) = v(h). \qquad \qquad \cdots (32)$$

Here $\sigma = \dfrac{h}{k^{1/2}}$ is the porous parameter. Then the kinematic condition (30) takes the form

$$v(h) = \frac{\partial\eta}{\partial t} + \left(1 + \alpha\,\sigma\frac{\eta}{h}\right)u(h)\frac{\partial\eta}{\partial x} . \qquad \cdots (33)$$

To obtain the equation for the interface elevation η, we find from eq. (6) the expression

$$v(h) = -\int_{0}^{h} \frac{\partial u}{\partial x}\, dy. \qquad \qquad \cdots (34)$$

The solution of (24), satisfying (27) and (28) is

$$u = \frac{1}{2\mu}\frac{\partial p}{\partial x}\left[y + h\frac{(\alpha\sigma - 2)}{1 - \alpha\sigma}\right]y, \ \alpha\,\sigma \neq 1. \qquad \cdots (35)$$

The case $\alpha\,\sigma = 1$ is treated in the last section. Then (33), using (29), (34) and (35) becomes

$$\frac{\partial\eta}{\partial t} + \frac{h^2\left(1 + \alpha\,\sigma\frac{\eta}{h}\right)}{2\mu\,(1 - \alpha\,\sigma)}\left[\delta\frac{\partial\eta}{\partial x} + \gamma\frac{\partial^3\eta}{\partial x^3}\right]\frac{\partial\eta}{\partial x} = \frac{h^3}{12\mu}\frac{(\alpha\,\sigma - 4)}{(1 - \alpha\,\sigma)}\left(\delta\frac{\partial^2\eta}{\partial x^2} + \gamma\frac{\partial^4\eta}{\partial x^4}\right) \quad \cdots (36)$$

Let us analyse the interface evolution described by this equation.

3.1 Linear Evolution of Interface

When η is very small, the nonlinear terms in eq. (36) are negligible and we get the linear equation

$$\frac{\partial \eta}{\partial t} = \frac{h^3}{12\mu} \frac{(\alpha \sigma - 4)}{(1 - \alpha \sigma)} \left(\delta \frac{\partial^2 \eta}{\partial x^2} + \gamma \frac{\partial^4 \eta}{\partial x^4} \right) \qquad \qquad \dots \text{(37)}$$

The question of interest is the growth rate of a small periodic perturbation of the interface. Hence we assume

$$\eta \, \alpha \exp{(nt + ilx)} \qquad \qquad \dots \text{(38)}$$

Then eq. (37), using eq. (38), becomes

$$n = \frac{h^3 l^2}{12\mu} \frac{(4 - \beta)}{(1 - \beta)} (\delta - \gamma l^2) \, , \qquad \qquad \dots \text{(39)}$$

where $\beta = \alpha \sigma$. In the limit $\beta \to 0$, eq. (39) reduces to

$$n = \frac{h^3 l^2}{3\mu} (\delta - \gamma l^2), \qquad \qquad \dots \text{(40)}$$

in agreement with the results of Babchin et al.[19] Although these authors discussed RTI of plane Couette flow, their evolution of the interface, in the case of linear theory, is independent of the velocity of the bounding plate, because their velocity distribution is independent of this velocity. The situation in the case of nonlinear evolution of the interface is quite different. In terms of non-dimensional quantities, eq. (39) takes the form

$$\hat{n} = \frac{\hat{h}^3 \hat{l}^2}{12} \frac{(4 - \beta)}{(1 - \beta)} (1 - \hat{l}^2) \, . \qquad \qquad \dots \text{(41)}$$

Here $\hat{n} = \frac{\mu n}{\sqrt{\gamma \, \delta}}, \quad \hat{l} = \lambda l. \qquad \hat{h} = h/\lambda. \qquad \qquad \dots \text{(42)}$

$\hat{n}$ given by eq. (41), is computed for different values of $\hat{l}, \hat{h}$ and β and the results are discussed in the last section.

3.2 Nonlinear Evolution of Interface

Eq. (41) shows that the interface is neutrally stable (i.e., $\hat{n}$ = 0), for values of β = 4. RT stability (i.e. n < 0) occurs for values of β in the range $1 < \beta < 4$ and shorter-scale perturbations $\left(l^2 < \frac{\delta}{\gamma} \right)$. Longer-scale $\left(l^2 > \frac{\delta}{\gamma} \right)$ perturbations amplify for values of β in the range $1 < \beta < 4$ and die out for $\beta > 4$. Shorter-scale perturbations $\left(l^2 < \frac{\delta}{\gamma} \right)$ are linearly unstable for values of $\beta > 4$ or $\beta < 1$ and thus subject for a nonlinear theory. We see that the characteristic length λ, eq. (14), is of the order of the critical wavelength. Eq. (41) shows that the growth-rate is maximum at a wavelength which is of the same order as λ. But, if η is very large, i.e. $\eta \gg hS$, then the linear terms in eq. (36) can be neglected and we obtain:

$$\frac{\partial \eta}{\partial t} + \frac{h^2\left(1 + \beta\frac{\eta}{h}\right)}{2\mu(1-\beta)}\left[\delta\frac{\partial \eta}{\partial x} + \gamma\frac{\partial^3 \eta}{\partial x^3}\right]\frac{\partial \eta}{\partial x} = 0. \qquad \text{... (43)}$$

The process described is quite different from a process in which the film is bounded by a fluid layer with moving boundaries instead of porous layer, discussed by Babchin et al.[19]. Therefore, we use eq. (36) to study the nonlinear interface evolution. Eq. (36) is not amenable to analytical treatment and hence we solve it numerically using 4th order central differences in space and time as explained below. For time-integration of eq. (36) Adams-Bashforth predictor and Adams-Moulton corrector steps of fourth order are used, as described in Chapra and Canale[21]. Spatial derivatives are discretized by the following central difference formulae of fourth order accuracy :

$$\frac{\partial \eta(x)}{\partial x} \mapsto \frac{1}{12\Delta x}[\eta(i-2) - 8\eta(i-1) + 8\eta(i+1) - \eta(i+2)], \qquad \text{... (44)}$$

$$\frac{\partial^2 \eta(x)}{\partial x^2} \mapsto \frac{1}{12\Delta x^2}[-\eta(i-2) + 16\eta(i-1) - 30\eta(i) + 16\eta(i+1) - \eta(i+2)], \qquad \text{... (45)}$$

$$\frac{\partial^3 \eta(x)}{\partial x^3} \mapsto \frac{1}{8\Delta x^2}[-\eta(i-3) - 8\eta(i-2) + 13\eta(i-1) - 13\eta(i+1) + 8\eta(i+2) - \eta(i+3)] \qquad \text{... (46)}$$

and
$$\frac{\partial^4 \eta(x)}{\partial x^4} \mapsto \frac{1}{6\Delta x^4}[-\eta(i-3) + 12\eta(i-2) - 39\eta(i-1) + 56\eta(i)$$

$$- 39\eta(i+1) + 12\eta(i+2) - \eta(i+3)]. \qquad \text{... (47)}$$

The abbreviated notation, e.g., $\eta(i-2)$, stands for the value of η at the position $x - 2\Delta x$. The integer 'i' indicates the i-th grid point.

The initial condition used in the numerical integration is a sine-wave with wavenumber l:

$$\eta(x, 0) = \eta_0 \sin(lx). \qquad \text{... (48)}$$

The amplitude η_0 is assumed small. Its non-dimensional value is $\hat{\eta}_0 = 10^{-4}$.

Periodic boundary conditions have been applied in x-direction.

4. LINEAR EVOLUTION OF INTERFACE USING ONLY STOKES APPROXIMATION

Using the approximations discussed in section 2 without the approximation (23), eqs. (5) and (6) take the form

$$\frac{\partial^2 u}{\partial x^2} + \frac{\partial^2 u}{\partial y^2} = \frac{1}{\mu}\frac{\partial p}{\partial x}, \qquad \text{... (49)}$$

$$\frac{\partial^2 v}{\partial x^2} + \frac{\partial^2 v}{\partial y^2} = \frac{1}{\mu}\frac{\partial p}{\partial y} \qquad \text{... (50)}$$

and $\qquad \dfrac{\partial u}{\partial x} + \dfrac{\partial v}{\partial y} = 0 \cdot$ ... (51)

The required boundary and interface conditions are given by eqs. (19) to (22). The question of interest, here also, is the growth rate of a small periodic perturbation of the interface. Hence, we assume :

$$(u, v, \eta) = (\tilde{u}(y), \tilde{v}(y), \tilde{\eta}\,(y))\ \exp\ (nt\ +\ ilx).$$ ... (52)

Substituting eq. (52) into eqs. (49) to (51) and simplifying (see Brown[17]), we get

$$D^4\,\tilde{v} - 2l^2\,D^2\,\tilde{v} + l^4\,\tilde{v} = 0,$$ ... (53)

where $\qquad D = \dfrac{d}{dy}\ .$

This has to satisfy the conditions

$$\tilde{v} = D\tilde{v} = 0\ \text{at}\ y = 0,$$ ... (54)

$$(D^2 + l^2)\tilde{v} = \dfrac{\alpha}{\sqrt{k}}\,D\tilde{v}\ \text{at}\ y = h$$ ... (55)

and $\qquad p = \dfrac{\mu}{l^2}\,(D^3\,\tilde{v} - l^2 D\,\tilde{v})\qquad \text{at}\quad y = h.$ ... (56)

The kinematic condition (22), after neglecting the second term in it (as it is of second order) becomes

$$\tilde{v}\,(h) = n\,\tilde{\eta}.$$ ... (57)

From (49) and (56), using (51) and (57), we get

$$n = \dfrac{l^2(\delta - \gamma l^2)\,\tilde{v}(h)}{\mu[2l^2\,D\,\tilde{v}(h) - D^3\,\tilde{v}(h)]}\ \cdot$$ ... (58)

Solution of eq. (53), satisfying the above conditions, is

$$\tilde{v}(y) = (A_2 + A_1 y)\sinh\,(ly) + (A_4 + A_3 y)\cos\,h(ly).$$ ... (59)

Here

$$A_4 = 0,\quad A_3 = -\dfrac{A_1}{lh}\,f,\quad A_2 = \dfrac{A_1}{l^2 h}\,f,$$

$$f = \dfrac{2lh(\dot{C} + lh\,\dot{S}) - \beta\,(\dot{S} + lh\,\dot{C})}{2lh\,\dot{C} - \beta\,\dot{S}}\ ,$$

$$\dot{C} = \cosh\,(lh),\quad \dot{S} = \sinh\,(lh).$$ ... (60)

So, the dispersion relation (58), using eq. (59), is given by

$$n = \frac{(\delta - \gamma l^2)}{\mu l} N \ . \qquad \qquad \cdots (61)$$

Here

$$N = \frac{\dot{S}\,\dot{C} - lh + \beta(2lh)^{-1}(l^2h^2 - \dot{S}^2)}{2\dot{C}^2 + l^2h^2 - \beta(1 + \dot{S}\,\dot{C})} \ . \qquad \qquad \cdots (62)$$

In the limit $\beta \to 0, N \to N_0$ where

$$N_0 \to \frac{\dot{S}\,\dot{C} - lh}{2\dot{C}^2 + l^2h^2} \ , \qquad \qquad \cdots (63)$$

$$n \to \frac{(\delta - \gamma l^2)N_0}{\mu l} \qquad \qquad \cdots (64)$$

is in agreement with the results of Brown[17]. (We note a printing mistake in the expression N_0 given by Brown [4], where we find $\dot{C}^2$ instead of $\dot{C}$ in the denominator of (63).)

Making the expression n given by eq. (61) dimensionless, using eq. (42), we get

$$\hat{n} = (\hat{l})^{-1}(1 - \hat{l}^2)\hat{N} \ . \qquad \qquad \cdots (65)$$

Here $\hat{N}$ is given by eq. (62) by replacing lh by $\hat{l}\hat{h}$.

$\hat{n}$ given by eq. (65) is computed for different values of $\hat{l}, \hat{h}$ and β and the results are discussed in the last section.

5. Discussion and Conclusions

In this paper, we have investigated linear and nonlinear Rayleigh-Taylor instability of two-dimensional flow in a rectangular comparatively thin fluid layer bounded above by a thick porous layer and below by a rigid plate. Using the approximations common in thin-film lubrication theory and in Stokes flow discussed in sections 3 and 4, we obtain the dispersion relations (39) and (58). Relation (39) is valid for $\beta \neq 1$. When $\beta \to 1$, we find that $\frac{\partial p}{\partial x} \to 0$ and the corresponding dispersion relation is

$$\hat{n} = \frac{\hat{h}^3 \hat{l}^2}{12}(1 - \hat{l}^2) \ . \qquad \qquad \cdots (66)$$

The dispersion relations (41) and (65) are numerically evaluated for different values of $\hat{l}, \hat{h}$ and β and the results are depicted in Figs. 2 and 3. We find that the shape of the dispersion curves as well as the nature of the linear stability of the interface depend on β and $\hat{h}$. In the case of a thin film bounded by a fluid layer, Babchin et al.[16] and Brown[17] have shown that the interface is always linearly unstable for long waves $\left(l^2 < \frac{\delta}{\gamma}, \text{ i.e. } \hat{l}^2 < 1 \right)$. However, in the problem discussed here the situation is quite different. For $\hat{l}^2 < 1$, solution (39) shows that the interface is neutrally stable (i.e. $n = 0$) for $\beta = 4$, that it is stable (i.e. $n < 0$) for values of β in the range $1 < \beta < 4$ and linearly
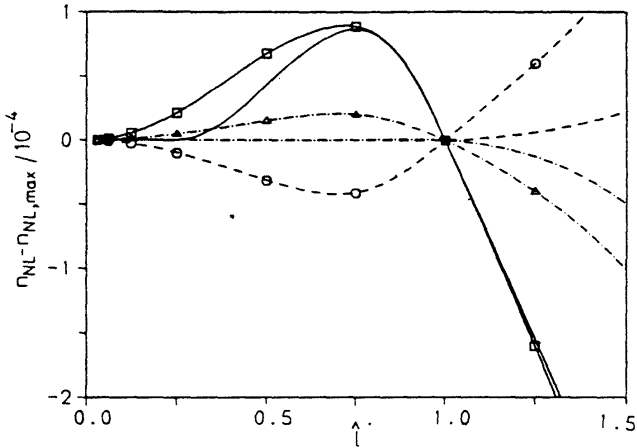
FIG. 2. Linear (curves with symbols) and nonlinear (simple curves) dispersion relations for three different values of $\beta = \alpha\sigma$ ($\beta = 0.1$: ——, $\beta = 2.0$: ——— $\beta = 100.0$: -.-.-) and a 'thin' fluid layer of thickness $h = 0.1\left(\dfrac{\gamma}{\delta}\right)^{\frac{1}{2}}$.
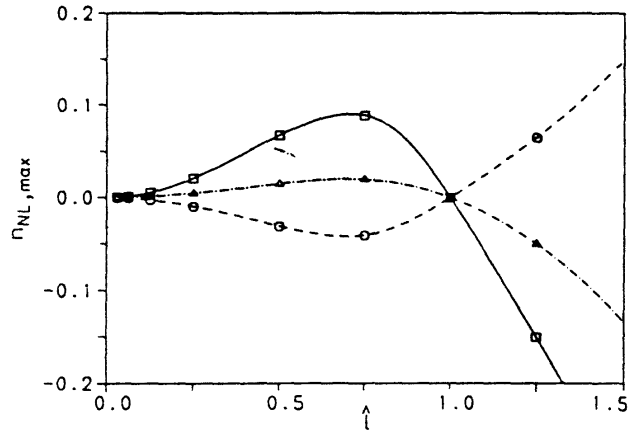
FIG. 3. Linear and nonlinear dispersion relations for three different values of $\beta = \alpha\sigma$ ($\beta = 0.1$: ----, $\beta = 2.0$: - - - , $\beta = 100.0$: -. -. - .) and a 'thick' fluid layer with $h = \left(\dfrac{\gamma}{\delta}\right)^{\frac{1}{2}}$. Linear and nonlinear results coincide.

unstable (i.e. $n > 0$) for $\beta > 4$ or $\beta < 1$. The opposite is true for short waves $\left(l^2 > \dfrac{\delta}{\gamma}, \text{resp.} \hat{l}^2 > 1 \right)$. The interface which is stable for long waves becomes unstable for short waves and vice versa. This means that the slip parameter greatly influences the nature of the interface as stated in the introduction. To demonstrate this by analytical and numerical tools is one of the motives of the present study.

In Figs. 2 and 3, we present not only linear, but also nonlinear results for two different values $\hat{h}$ of the fluid layer, namely $\hat{h} = 0.1$ and 1 and three values of the parameter $\beta = \alpha\sigma = 0.1$, 2.0, 100.0, which are representative of the parameter ranges discussed above. While the linear results are characterized by curves with the symbols $\square$ O $\triangle$, the nonlinear results are represented by simple curves (solid, dashed and dashed-dotted). In the case of linear results, the vertical axes of Figs. 2, and 3 represent the growth rate $\hat{n}$ of the interface perturbation $\hat{\eta}$ (cf. ef. (41)). In the nonlinear cases it provides the relative time rate of change of $\hat{\eta}_{max}$, namely $\dfrac{1}{\hat{\eta}_{max}}\dfrac{\partial\hat{\eta}_{max}}{\partial t}$. $\hat{\eta}_{max}$ denotes the maximum nondimensional perturbation of the interface. It turns out the both quantities coincide perfectly for 'thick' fluid layers, given e.g. by $\hat{h} = 1.0$, i.e. $h = \left(\dfrac{\gamma}{\delta}\right)^{\frac{1}{2}}$ (Fig. 3). In other words: if the thickness of the fluid layer is of the order of $\left(\dfrac{\gamma}{\delta}\right)^{\frac{1}{2}}$, the interface evolves linearly. On the other hand, thin fluid layers (e.g. $\hat{h} = 0.1$, see Figure 2) are more sensible to buoyancy and/or surface tension effects and undergo a nonlinear temporal evolution, irrespective of the wavenumber $\hat{l}$. Again $\hat{l} = 1$ represents a special case. We also conclude from Figs. 2 and 3 that the shape of the 'dispersion

curves in the linear and nonlinear cases is controlled by the porous parameter β alone. There are no qualitative differences between 'thick' and 'thin' fluid layers. When $\hat{h}$ becomes very large, however, the approximations in section 3 are invalid.
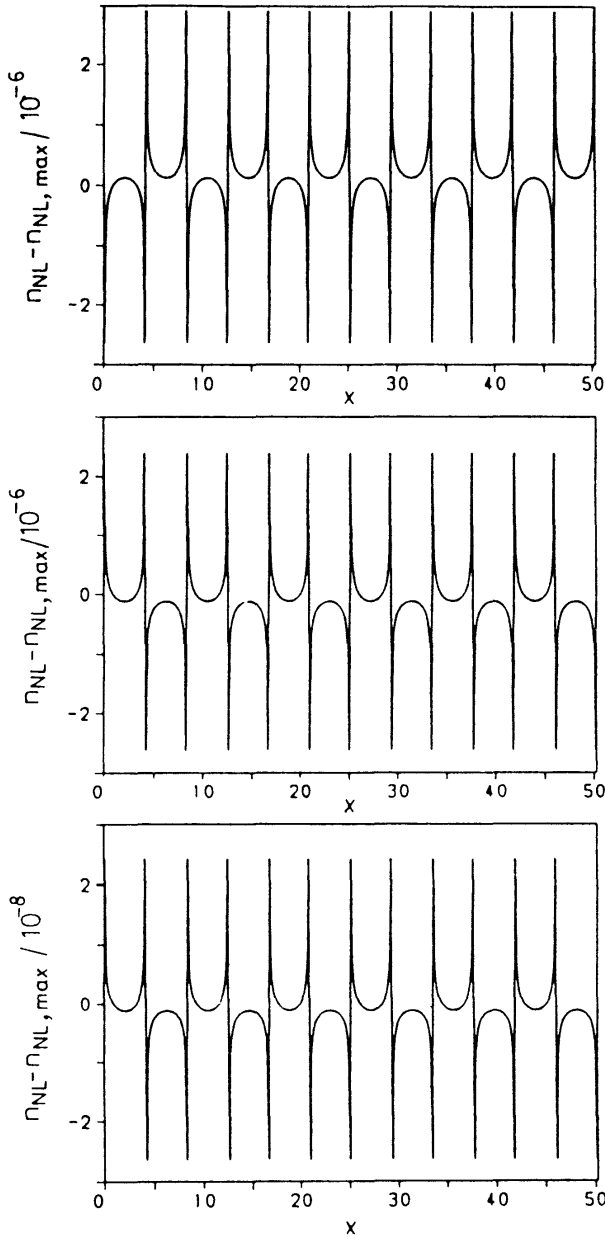

FIG. 4. Shape of interface growth rate for a wave-number of $\hat{l} = 0.75$ and three porous parameters $\beta = 0.1, 2.0, 100.0$ (from top to bottom).
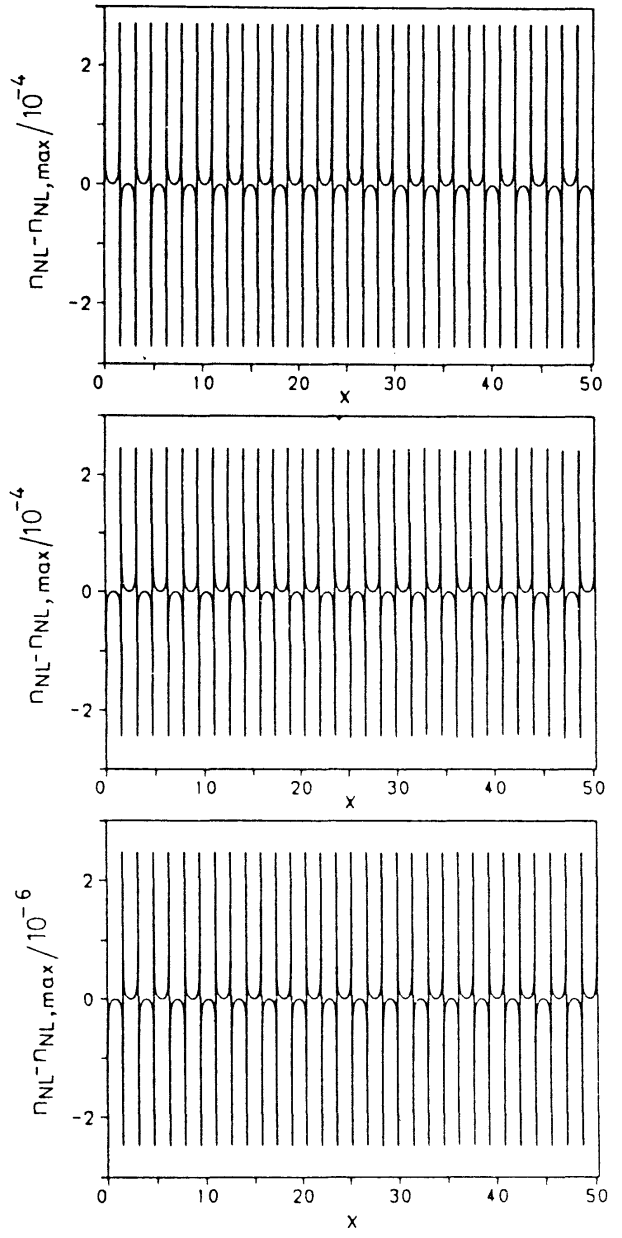
FIG. 5. Shape of interface growth rate for a wavenumber of $\hat{l} = 2.0$ and three porous parameters $\beta = 0.1, 2.0, 100.0$ (from top to bottom).

Finally, it is interesting to discuss the spatial structure of the relative growth rate of the interface in Figs. 4 and 5 in terms of the quantity $n_{NL} - n_{NL, \max} = \dfrac{1}{\hat{\eta}} \dfrac{\partial \hat{\eta}}{\partial \hat{t}} - \dfrac{1}{\hat{\eta}_{\max}} \dfrac{\partial \hat{\eta}_{\max}}{\partial \hat{t}}$ at an early stage, before instability occurs for two wavenumbers $\hat{l} = 0.75$ and 2.0 and the three porous parameters

β selected in Figs. 2 and 3. In fact, the instant of time considered in these thin layer results is $\hat{t}$ = 5.10^{-4} and thus close to the initial time. In Fig. 4, six waves are contained in the interval 16π. The peaks reflect the positions of the wave modes. Since $n_{NL, max} \approx 0$ for β = 100, the peaks are the positions where the growth rate is maximum. This is not true for β = 0.1 and 2.0, where the positions for $n_{NL, max}$ coincide with those of the wave crests. The case of large wavenumber is presented in Fig. 5. Now 16 complete waves are stored in the interval 16π. Compared to the $\hat{t}$ = 0.75-case the amplitudes have increased, but the shapes of the interface growth rates are qualitatively
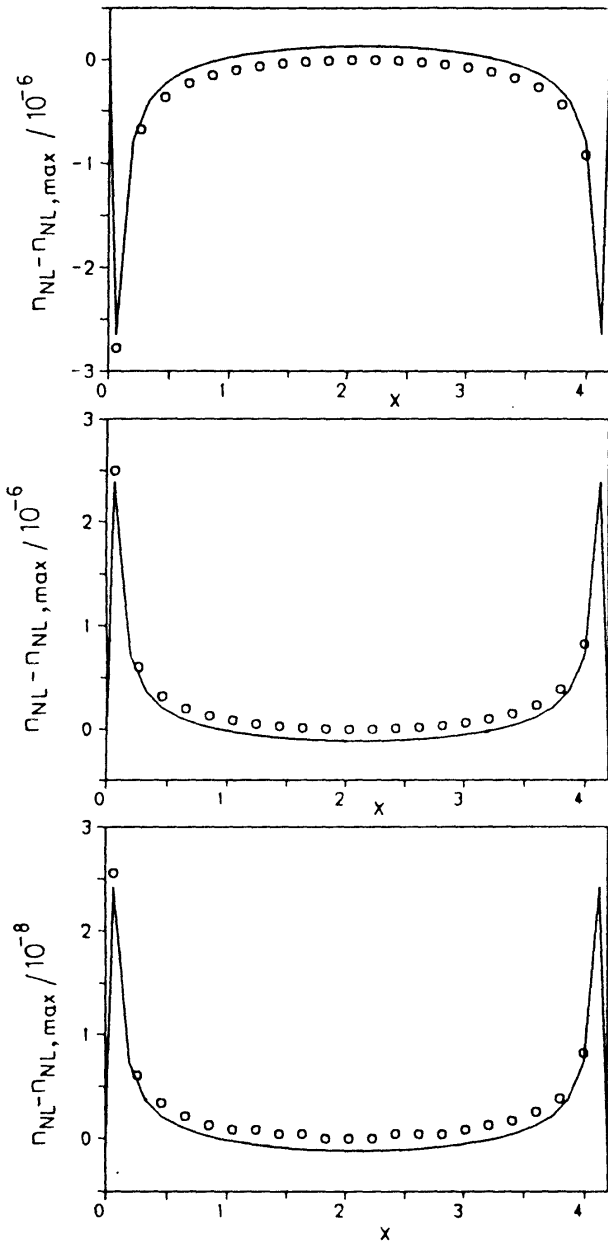

FIG. 6. Comparison between full numerical solutions of eq. (36) and solutions with presumed spatial structure (symbols) for a long wave with $\hat{t}$ = 0.75 and for the three porous parameters β = 0.1, 2.0 and 100.0 (from top to bottom).
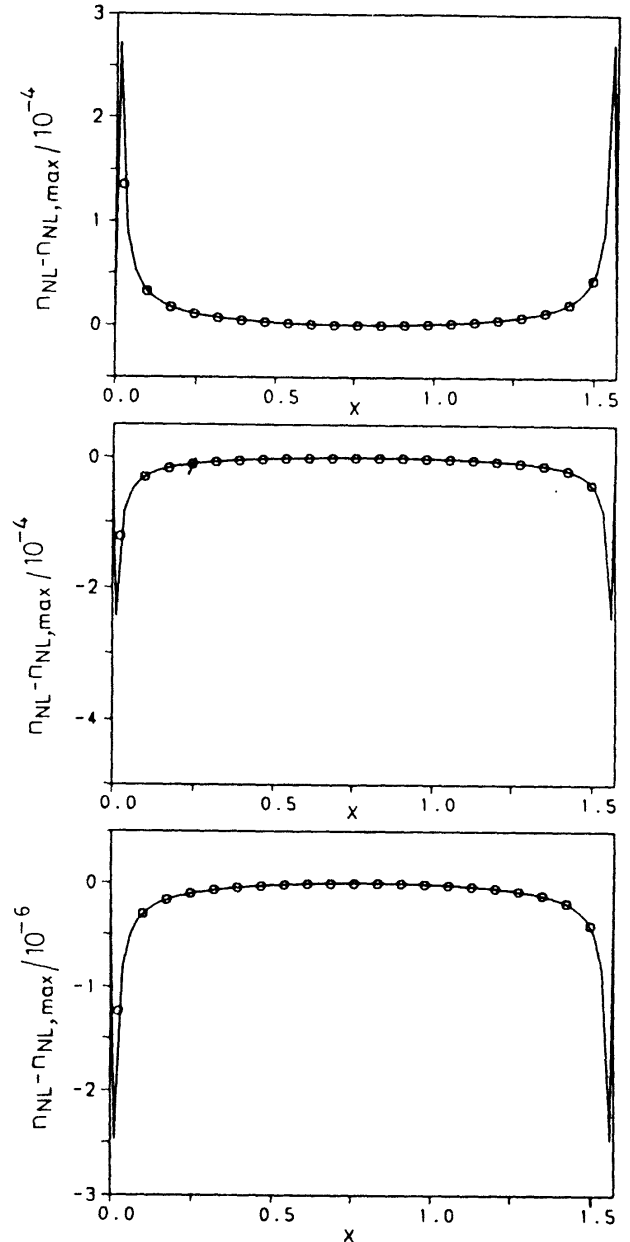
FIG. 7. Comparison between full numerical solutions of eq. (36) and solutions with presumed spatial structure (symbols) for a short wave with $\hat{t}$ = 2.0 and for the three porous parameters β = 0.1, 2.0 and 100.0 (from top to bottom)

the same. Whether the full numerical solutions deviate from a simple harmonic behaviour of η, namely $\eta(x, t) = \eta_0(t) \sin(lx)$, is demonstrated in Figs. 6 and 7, where half waves are shown only and the solid curves represent the general nonlinar case and the dashed curves the case with presumed spatial structure of η, introduced into eq. (36). Indeed, the general solutions are close to simple harmonic waves for long and short waves ($\hat{l} = 0.75$, 2.0) and all porous parameters, at least during the short time interval considered. Computations at later times became unstable. The presumed solution deviates earlier from the general solution when the wavenumber is small.

In conclusion, the nonlinear problem discussed here (section 3.2) is quite different from that of Babchin et al.[19] considering plane Couette flow. The present problem is greatly influenced by the slip velocity at the interface between porous layer and thin film. It is not amenable to analytical treatment as that of Babchin et al.[19]. Therefore, numerical solutions had to be found. Fourth-order accurate central differences were used for spatial discretization. For large porous parameters of the order of $\sigma = 10^4$, however, it was not possible to obtain smooth solutions. Instead, chaotic but bounded solutions appeared which could not be avoided by increasing the number of grid points even dramatically. A remedy might be to use upwind discretizations or to add artificial viscosity terms to the centrally discretized terms.

REFERENCES

1. Lord Rayleigh. *Scientific Papers, Cambridge*, England, VOl. II: 200-207, (1900)

2. G. I. Taylor, *Proc. R. Soc. London*, **A201** (1950) 192-196.

3. S. Chandrasekhar, *Hydrodynamic and Hydromagnetic Stability*, Oxford University Press, Clarendon Press, Oxford (1961)

4. D. H. Sharp, *Physica* **12(D)** (1984) 3-18.

5. K. O. Mikaelian, *Phys. Rev. E*, **47**(1) (1993) 375-382.

6. I. B. Bernstein and D. L. Book, *Phys. Fluid.*, **26**(2) (1983) 453-458

7. K. O. Mikaelian, *Phys. Rev. A.* **46**(20) (1992) 6621-6627

8. N. Rudraiah, B. S. Krishnamurthy and R. D. Mathod, *Acta Mechanica* **92** (1995) 220-240

9. N. Rudraiah, In: *Proc. II Asian Congress of Fluid Mechanics*, pages 1015-1020 (1983) Science Press Beijung, China

10. N. Rudraiah, Heat and mass transfer in composite materials. *Presidential Address*. Mathematics Section of 76th Session of the Indian Science Congress Association, Madurai University, Madurai, India (1989).

11. V. Prasad, In: Kakac *et al.* (ed.) *Convective Heat and Mass Transfer in Porous Media*, pages 563-615. Kluwer Academic Publishers (Nethrlands), (1991).

12. G. S. Beavers and D. D. Joseph, *J. Fluid Mech.*, **30** (1967) 197-207

13. G. I. Taylor, *J. Fluid Mech.*, **49** (1971) 319-326

14. S. Richardson, *J. Fluid Mech.*, **49** (1971) 327-336

15. P. G. Saffman. *Stud. Appl. Math.* **50** (1971) 93-101

16. N. Rudraiah, *J. Fluids Enng.* **107** (1985) 322-329

17. H. C. Brown, *Phys. Fluid.* **A.1**(5) (1989) 895-896.

18. Y. Ognewicz and C. L. Tien, *Int. J. Hat Mass Transfer*, **24**(1981) 421-429

19. A. J. Babchin, A. L. Frankel, B. G. Levich, and G. I. Sivashinsky, *Phys. Fluids*, **26** (1983) 3159-3161

20. D. Vortmeyer and J. Schuster. *Chem. Engng. Sci.* **38**(10) (1983) 1691-1699

21. St. C. Chopra and R. P. Carale, Numerical methods for engineers McGrow-Hill publ. corp. New York, 2nd Edition, 1998